Quantum Electronics **35** (7) 658 – 662 (2005)

PACS numbers: 42.65.Hw; 42.65.Sf; 42.70.Nq
DOI: 10.1070/QE2005v035n07ABEH008956

Features of the dynamics of self-pumped loop phase-conjugate mirrors based on a photorefractive crystal

Mehran Vahdani Mogaddam, V.V. Shuvalov

***Abstract*. It is shown by numerical simulations that the nonlinear reflection coefficient of a loop phase-conjugate (PC) mirror based on a $BaTiO_3$ photorefractive crystal achieves under optimal conditions the maximum value 0.80 – 0.90 at the maximum overlap integral equal to 0.90 – 0.95. The conjugate wave is generated in such a mirror due to scattering from a dynamic hologram produced in the self-intersection region of the forward and backward beams. As a result, the scenario of passing to unstable generation regimes in this case substantially differs from that described earlier for a single-crystal double PC mirror.**

Keywords: *loop PC mirror, photorefractive nonlinearity, conjugate-wave formation dynamics, stable and unstable generation regimes.*

1. Introduction

Phase distortions caused by optical inhomogeneities can be compensated by using the so-called nonlinear phase-conjugate (PC) mirrors based on photorefractive crystals (PRCs) [1]. Such mirrors can operate at cw radiation intensities up to a few mW cm^{-2} [2]. Moreover, some of them do not require any pump sources (self-pumped double and loop PC mirrors, PC mirrors with a linear resonator, etc.) [3], being in fact threshold-free (with respect to the radiation intensity but not to the nonlinear interaction constants) and sometimes mirror-free parametric oscillators. For example, in the so-called single- and two-crystal double PC mirrors [4], two certainly non-interfering (incoherent or having different frequencies) light waves are simultaneously conjugated. The development of generation in this case is a classical example of self-organisation proceeding in the nonlinear medium – light field system. By varying the parameters and geometry of the problem, the response time τ can be changed from a few tens of seconds to milliseconds and less [5] or quite complicated self-oscillation (dynamic) generation regimes can be obtained with the characteristic times up to a few hours and days [2].

It was shown in [6] that in a single-crystal double PRC PC mirror, along with a dynamic hologram formed in the self-intersection region of input beams, the additional refractive-index gratings are produced in the interaction geometry typical of two-crystal PC mirrors. A competition between these two PC channels leads to a complicated spatiotemporal dynamics of generated nonlinear waves. Both the generation of two conjugate waves with the efficiency up to 70 % – 80 % and the appearance of a resemblance of dynamic chaos in a system of thin soliton-like filaments become possible. Our numerical simulations presented below show that there is no competition between several PC channels of this type in loop PC mirrors and the scenario of passing to unstable generation regimes substantially differs from that described in [6].

Mehran Vahdani Mogaddam, V.V. Shuvalov Department of Physics, M.V. Lomonosov Moscow State University, Vorob'evy gory, 119992 Moscow, Russia; e-mail: vsh@phys.msu.ru

Received 31 March 2005
Kvantovaya Elektronika **35** (7) 658 – 662 (2005)
Translated by M.N. Sapozhnikov

2. Model of a loop PC mirror

Figure 1 illustrates the geometry of the model problem. We assume that the forward light wave with the amplitude A_f and the wave vector $\boldsymbol{k} = \{k_x, k_z\}$ propagates from the input face of a PRC (the $z = 0$ plane) at a small angle ($k_z \gg k_x$) $\alpha/2$ in the positive direction of the z axis. The wave-front tilt is accounted for in the expression for $A_f(x, z = 0, t)$ by the phase factor $\exp[ikx \sin(\alpha/2)]$. It is assumed that an optical system consisting of two fold mirrors M1 and M2 and lens L, which forms the backward wave (propagating in the negative direction of the z axis) with the amplitude A_b,

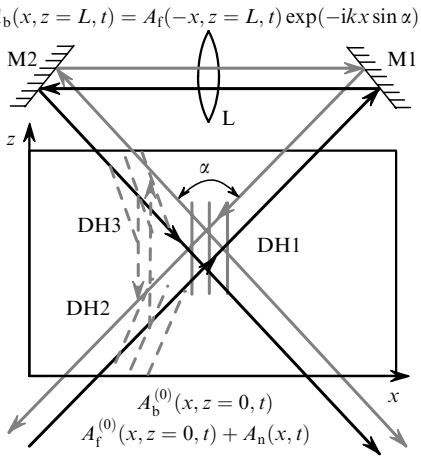

Figure 1. Interaction geometry of the waves $A_{f,b}(x, z, t)$ in a loop PC mirror: DH1, DH2, and DH3: dynamic holograms for the first (DH1, the self-intersection region) and second (DH2 and DH3, see [6]) possible generation channels; L: the PRC length.

is mounted directly behind the output face of the PRC (the $z = L$ plane). The mirrors changed the propagation direction of the wave A_f by the angle $(\pi - \alpha)$, while the lens transferred the image (the A_f field distribution) of the output face of the PRC. This provided the fulfilment of the boundary condition $A_b(x, z = L, t) = A_f(-x, z = L, t) \times \exp(-ikx \sin\alpha)$.

The nonlinear response of the PRC was calculated by using a classical system of microscopic equations [7] for the two-dimensional case taking into account transmission dynamic holograms (the grating vector is directed along the x axis) [1] and neglecting the photovoltaic effect:

$$\frac{\partial n}{\partial t} = \frac{\partial N_d^+}{\partial t} - \frac{1}{e}\frac{\partial j}{\partial x},$$

$$\frac{\partial N_d^+}{\partial t} = s(I + I_0)(N_d - N_d^+) - \gamma_r n N_d^+, \qquad (1)$$

$$j = e\mu n(E_0 + E_{sc}) - \mu\Theta\frac{\partial n}{\partial x},$$

$$\frac{\partial E_{sc}}{\partial x} = \frac{4\pi e}{\varepsilon}(n + N_a - N_d^+).$$

Here, n, N_a, N_d, and N_d^+ are the concentrations of free carriers, acceptors, and neutral and ionised donors; s is the photoionisation cross section; $I(x, t)$ is the light intensity; I_0 describes the intrinsic conductivity of the PRC by defining the rate of dark photoionisation as sI_0; γ_r is the recombination constant; e and μ are the charge and mobility of free carriers taking the carrier sign into account ('$-$' for electrons and '$+$' for holes); $E_{sc}(x, t)$ is the electrostatic intra-crystal field; ε is the quasi-static permittivity; and Θ is the temperature in energy units. It is assumed that the external electric field E_0 is applied to the PRC in the transverse direction (along the x axis). Therefore, system (1) takes into account both the drift and diffusion components of the current density vector $\boldsymbol{j}$ only in one direction.

System (1) was solved together with standard truncated wave equations for the complex amplitudes $A_{f,b}(x, z, t)$ of light waves

$$\pm i\frac{\partial A_{f,b}}{\partial z} = \frac{1}{2k}\frac{\partial^2 A_{f,b}}{\partial x^2} + k\frac{\delta\eta}{\eta}A_{f,b} \mp i\alpha_a A_{f,b}. \qquad (2)$$

Here, $k = 2\pi\eta/\lambda$ is the wave number; η is the refractive index of the PRC; λ is the wavelength; $\delta\eta = -\frac{1}{2}r_{eff}\eta^3 E_{sc}(x, t)$ is the nonlinear addition to η; r_{eff} is the effective electro-optic coefficient; and α_a is the absorption coefficient. Equation (2) is written in the paraxial approximation by omitting a spatially homogeneous addition to η. Equations (1) and (2) form the self-consistent problem that takes into account the relation between the distributions of the light intensity $I(x, z, t) = |A_f(x, z, t)|^2 + |A_b(x, z, t)|^2$ and the field $E_{sc}(x, t)$. This model describes the interaction of the so-called slit beams, which are often used in experiments with PRCs due to a strong anisotropy of the nonlinear response of these crystals [8].

It was shown in [9] that when $N_a \gg n$, $I_0 \gg I$, and $a\partial E_{sc}/\partial x \ll 1$, during the formation of the spatial spectrum of the field $E_{sc}(\kappa)$, the PRC plays the role of a filter of spatial frequencies with the transfer function

$$T(\kappa) = -\frac{E_0}{I_0}\frac{1 + i\kappa\Theta/(eE_0)}{1 - i\kappa a E_0(\chi + 1) + \kappa^2 a\Theta(\chi + 1)/e} \qquad (3)$$

with respect to the spatial spectrum of the intensity distribution $I(\kappa)$. Here,

$$a = \frac{\varepsilon}{4\pi e N_a}, \quad \chi = \frac{N_a}{N_d - N_a}. \qquad (4)$$

By using the approach similar to [9], one can easily show that the spectrum of the field $E_{sc}(\kappa, \Omega)$ in transient problems is determined by the spatiotemporal spectrum of the intensity distribution $I(\kappa, \Omega)$, while the PRC becomes a spatiotemporal filter with the transfer function

$$T(\kappa, \Omega) = -\frac{E_0}{I_0}\frac{1 + i\kappa\Theta/(eE_0)}{1 - i\kappa a E_0(\chi + 1) + \kappa^2 a\Theta(\chi + 1)/e - i\Omega\tau_{di}}, \qquad (5)$$

where Ω is the frequency of oscillations of the corresponding component of the spatial spectrum of the intensity $I(\kappa, \Omega)$ and $\tau_{di} = \varepsilon\gamma_r\chi/(4\pi e\mu s I_0)$ is the dielectric relaxation time. A similar approach to the description of transient processes and dynamic regimes of PRCs was used in papers [10, 11].

We performed all the estimates and calculations for one of the most efficient and popular PRCs – barium titanate ($BaTiO_3$) with parameters listed below [5]:

sI_0/s^{-1}	4.0×10^{-5}
N_a/cm^{-3}	2.0×10^{17}
N_d/cm^{-3}	2.0×10^{18}
$s/cm^2\ W^{-1}s^{-1}$	0.67
$\mu/cm^2\ W^{-1}s^{-1}$	5.0×10^{-1}
$r_{eff}/cm\ V^{-1}$	9.7×10^{-7}
$\gamma_r/cm^3\ s^{-1}$	1.0×10^{-9}
ε	135
η	2.4
α_a/cm^{-1}	0.1

3. Scheme of numerical calculations

Dynamic holograms produced in a PRC upon phase conjugation can be adequately numerically described only by using extremely fine-mesh (with the cell size much smaller than the light-wave wavelength, $\Delta h \ll \lambda$) spatial-coordinate grids. This problem is aggravated in the analysis of dynamic regimes, when the required time step Δt is proportional to the square of Δh. That is why the numerical simulation of processes proceeding in PRCs is usually performed either in the quasi-stationary approximation [12] or by using rigid restrictions imposed on the spatial spectra of the interacting waves [13]. The dynamics predicted within the framework of such assumptions cannot correspond to real situations, which was confirmed in fact by experiments [14].

The self-consistent problem (1), (2) was solved by calculating numerically the evolution of spatial distributions of the complex amplitudes $A_{f,b}(x, z, t)$ of light waves and the nonlinear addition $\delta\eta(x, z, t)$ to the refractive index of the PRC in the geometry shown in Fig. 1. All the variables were described discretely (the number of the grid nodes of the PRC aperture $H = 4$ mm was 8192 and on its length $L = 4$ mm – 512). This means in fact that we were solving the problem of the nonlinear interaction of many plane waves (modes), whose total number is determined by the total number of the nodes of our grid along the x axis.

Although both the reflection and transmission dynamic holograms should be written during the interaction of counterpropagating light waves in the PRC [5], we considered only the transmission holograms (see above). In real experiments, this corresponds to situations when the counterpropagating light waves do not interfere, i.e., either they have already lost their coherence or are orthogonally polarised (an additional polarisation rotator is introduced into the M1 – L – M2 feedback loop). The initial conditions for all realisations corresponded to the PC mirror switching on at the instant $t = 0$. After that (for $t \geqslant 0$), the input field $A_f(x, z = 0, t)$ was assumed specified by a linear superposition of the stationary regular useful signal $A_f^{(0)}(x, z = 0)$ and the complex white noise $A_n(x, z = 0, t)$ delta-correlated in t (taking the time step Δt into account), whose average intensity $\langle I_n \rangle$ was varied between 10^{-3} and 10^{-6} of the maximum intensity I_{max} of the useful signal.

The evolution of the system was calculated by using the standard adiabatic approach [10, 11] assuming that the 'fast' subsystem (light field) instantly (adiabatically) follows all variations proceeding in the 'slow' subsystem (PRC). The complex amplitude $A_{f,b}(x, z, t)$ was calculated by assuming that the distribution $\delta\eta(x, z, t)$ is specified. Therefore, each calculation step was formally divided into two stages (Fig. 2). Each ith step in time (instant t_i) was started (the arrow WE in Fig. 2) from the calculation of the instant distributions $A_{f,b}(x, z, t_i)$ and $I(x, z, t_i)$ in the PRC by substituting into (2) the distribution $\delta\eta(x, z, t_{i-1})$ found at the previous step (instant t_{i-1}). The method of division over physical factors was used [10, 11]. The inhomogeneity of the refractive-index distribution was taken into account by transmitting both light waves successively through infinitely thin phase screens with the phase shifts specified by $\delta\eta(x, z = z_j, t_{i-1})$ and the grid step over z. Here, $j = 1, 2, ..., 512$ are the screen number. Diffraction effects were taken into account only during the propagation of light waves between the screens. At this stage, the fast Fourier transform was used. Then, the system of equations (1) was solved for the distribution $I(x, z, t_i)$ found in this way, and the distributions $E_{sc}(x, z, t_i)$ and $\delta\eta(x, z, t_i)$ (arrows ME and EO in Fig. 2) required for the passage to the next $(i + 1)$ step (instant t_{i+1}) were determined.

The time step was chosen to be much smaller that the characteristic evolution time of the PRC state (slow subsystem) $\Delta t = 0.1$ s because even small transformations of the dynamic hologram drastically changed the output-field distribution.

4. Results of numerical calculation

We assumed in our simulations that most of the parameters of the problem were determined by the selected PRC and were not varied. The intensity distribution $|A_f^{(0)}(x, z = 0, t)|^2$ of the signal radiation at a wavelength of 0.514 μm on the input face of the PRC was assumed Gaussian (the beam width was $2\rho_0 = 100$ μm) for $I_{max} = 2 - 200$ mW cm^{-2}. The period of dynamic hologram DH1 written in the PRC with the input aperture $H = 4$ mm and length $L = 4$ mm was varied by changing the convergence angle α of the beams within $10^\circ - 15^\circ$. The external electrostatic field strength E_0 was varied from 1 to 1000 V cm^{-1}.

The loop PC mirror was easily actuated [i.e., the generation of the field $A_b(x, z, t)$ with the spatial structure $A_b(x, z = 0, t)$ close to that of the conjugated input signal $A_f(x, z)$ was achieved]. Figure 3 shows the 'maps' of the intensity distributions $I_f(x, z)$ (Fig. 3a) and I_b (Fig. 3b) in the PRC already after the end of the transient process ($t = 1000$ s). Here, as in Fig. 6, the darker regions correspond to lower intensities. A stationary refractive-index grating DH1 was formed in the self-intersection region of the forward (A_f) and backward (A_b) beams in the PRC. Under optimal conditions (see below), the PC mirror completely transferred to the output (the $z = 0$ plane) the regular spatial intensity modulation introduced for control in the useful signal $A_f^{(0)}(x, z = 0)$ (Figs 3c, d). In this case,

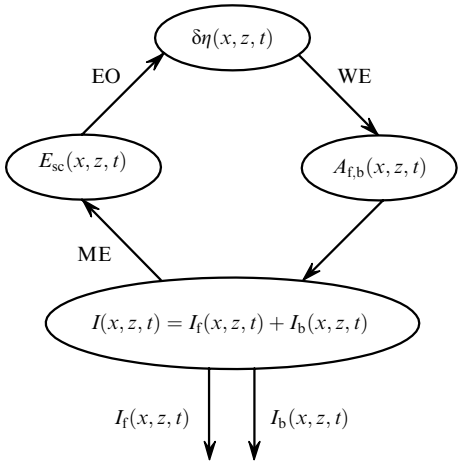

Figure 2. Solution of the self-consistent problem at each calculation step: WE: the calculation of $A_{f,b}(x, z, t)$ and $I(x, z, t) = I_f(x, z, t) + I_b(x, z, t)$ for the specified $\delta\eta(x, z, t)$ (wave equation); ME: the calculation of $E_{sc}(x, z, t)$ (constitutive equations); EO: the calculation of $\delta\eta(x, z, t)$ caused by the electro-optic effect.

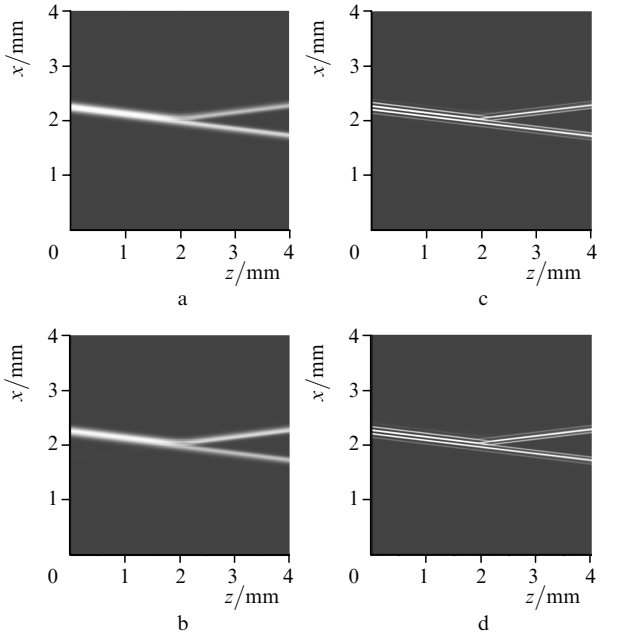

Figure 3. Maps of the distributions $I_f(x, z)$ (a, c) and $I_b(x, z)$ (b, d) at the instant $t = 1000$ s upon stationary phase conjugation of a Gaussian beam without the harmonic modulation of the input intensity $I_f(x, z = 0)$ (a, b) and in its presence (c, d); $\alpha = 14^\circ$, $I_{max} = 35$ mW cm^{-2}, $\langle I_n \rangle / I_{max} = 10^{-4}$, $E_0 = 1$ V cm^{-1}.

the overlap integral

$$H(t) = \frac{\left| \int_0^H A_f(x, z = 0, t) A_b^*(x, z = 0, t) \mathrm{d}x \right|^2}{\int_0^H |A_f(x, z = 0, t)|^2 \mathrm{d}x \int_0^H |A_b(x, z = 0, t)|^2 \mathrm{d}x} \quad (7)$$

on the input face of the PRC achieved the maximum value $H_{max} = 0.90 - 0.95$ for the nonlinear reflection coefficient

$$R(t) = \frac{\int_0^H |A_b(x, z = 0, t)|^2 \mathrm{d}x}{\int_0^H |A_f(x, z = 0, t)|^2 \mathrm{d}x}, \quad (8)$$

whose maximum value was $R_{max} = 0.80 - 0.90$ [curves (*1*) and (*4*) in Fig. 4]. Note that $H(t)$ and $R(t)$ were calculated by transmitting preliminary the output wave $A_b(x, z = 0, t)$ through a spatial filter, which selected half the linear aperture of the PRC corresponding to the position of the intensity maximum of the beam A_f in the $z = 0$ plane.

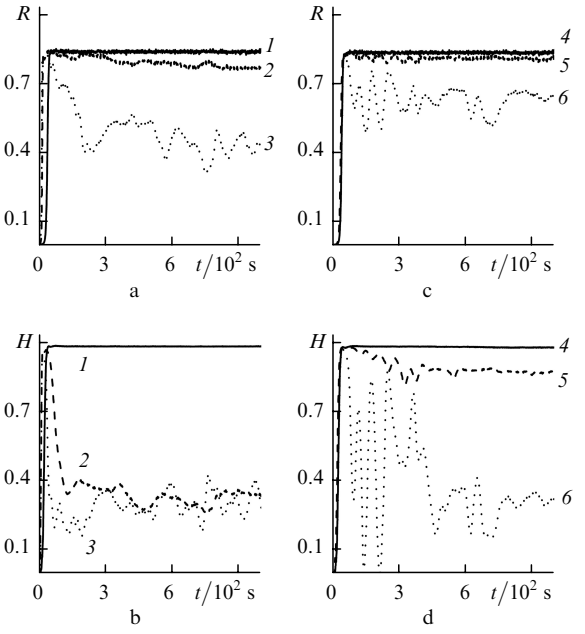

Figure 4. Transformation of the dependences $R(t)$ (a, c) and $H(t)$ (b, d) upon variations of the input-beam intensity I_{max} and the static electric field strength E_0 for $E_0 = 1$ V cm^{-1}, $I_{max} = 35$ (*1*), 70 (*2*), and 105 mW cm^{-2} (*3*) (a, b) and $I_{max} = 35$ mW cm^{-2}, $E_0 = 1$ (*4*), 175 (*5*), and 200 V cm^{-1} (*6*) (b, d); $\alpha = 14^\circ$, $\langle I_n \rangle / I_{max} = 10^{-4}$.

The time during which the phase transition occurred in the PC mirror (the appearance of the conjugate component of the input field at the output) depended on the convergence angle α of the beams and the relative noise level $\langle I_n \rangle / I_{max}$ of the input radiation A_f (Fig. 5). As α (Figs 5a, b) and $\langle I_n \rangle / I_{max}$ (Figs 5c, d) were increased in the ranges under study, the conjugate component formed faster. The change in the growth kinetics of R and H in time upon variations of the parameters α and $\langle I_n \rangle / I_{max}$ was different. As α was increased, the phase transition began earlier, i.e., both the overlap integral H (Fig. 5b) and the reflection coefficient R (Fig. 5a) faster achieved their maxima H_{max} and R_{max}, respectively. At the same time, the increase in $\langle I_n \rangle / I_{max}$ almost did not affect the dependence $H(t)$ (Fig. 5d), while

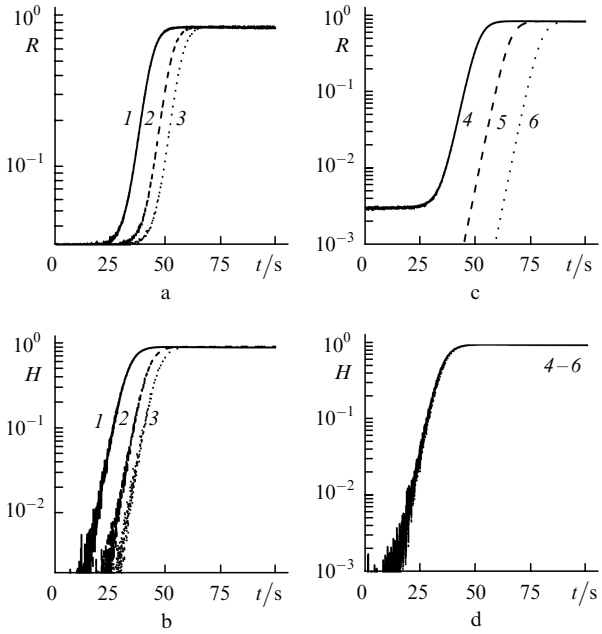

Figure 5. Delay of the PC mirror start with decreasing the convergence angle α and the relative noise level $\langle I_n \rangle / I_{max}$. Dependences $R(t)$ (a, c) and $H(t)$ (b, d) for $\langle I_n \rangle / I_{max} = 10^{-3}$, $\alpha = 15^\circ$ (*1*), 14° (2), and 12° (*3*) (a, b) and $\alpha = 14^\circ$, $\langle I_n \rangle / I_{max} = 10^{-4}$ (*4*), 10^{-5} (*5*), and 10^{-6} (*6*) (c, d); $I_{max} = 35$ mW cm^{-2}, $E_0 = 1$ V cm^{-1}.

$R(t)$ rapidly achieved the maximum value R_{max} only due to the increase in the amplitude of the initial noise seed (Fig. 5c).

As the input-beam intensity I_{max} [curves (*2*), (*3*) in Figs 4a, b] and the strength E_0 of the static electric field applied to the PRC [curves (*5*), (*6*) in Figs 4c, d] were increased, the efficiency and, which is more important, stability of phase conjugation drastically decreased. In the forward and backward beams, a complicated irregular system of thin soliton-like filaments began to appear gradually due to self-action (Fig. 6), in which then a resemblance of dynamic chaos appeared. In this case, many additional dynamic holograms were produced in the PRC due to numerous self- and mutual intersections of the filaments, and phase conjugation was no longer efficient.

5. Conclusions

We have presented the results of numerical simulation of the formation kinetics of a conjugate wave in a loop PC mirror based on a $BaTiO_3$ PRC. It is shown that the nonlinear reflection coefficient of such a mirror can achieve the maximum value $R_{max} = 0.80 - 0.90$ for the overlap integral value up to $H_{max} = 0.90 - 0.95$. The scenario of passing to unstable generation regimes in the loop PC mirror substantially differs from that described earlier [6] for a single-crystal double PC mirror. First of all this is explained by the fact that no competition can occur between several generation channels of the conjugate wave in the loop PC mirror. If the conjugate wave is generated in the mirror, this is certainly related to scattering from the dynamic hologram DH1 (Fig. 1) produced in the self-intersection region of the forward and backward beams. The DH2 and DH3 gratings are produced in the loop PC mirror only in the unstable generation regime,

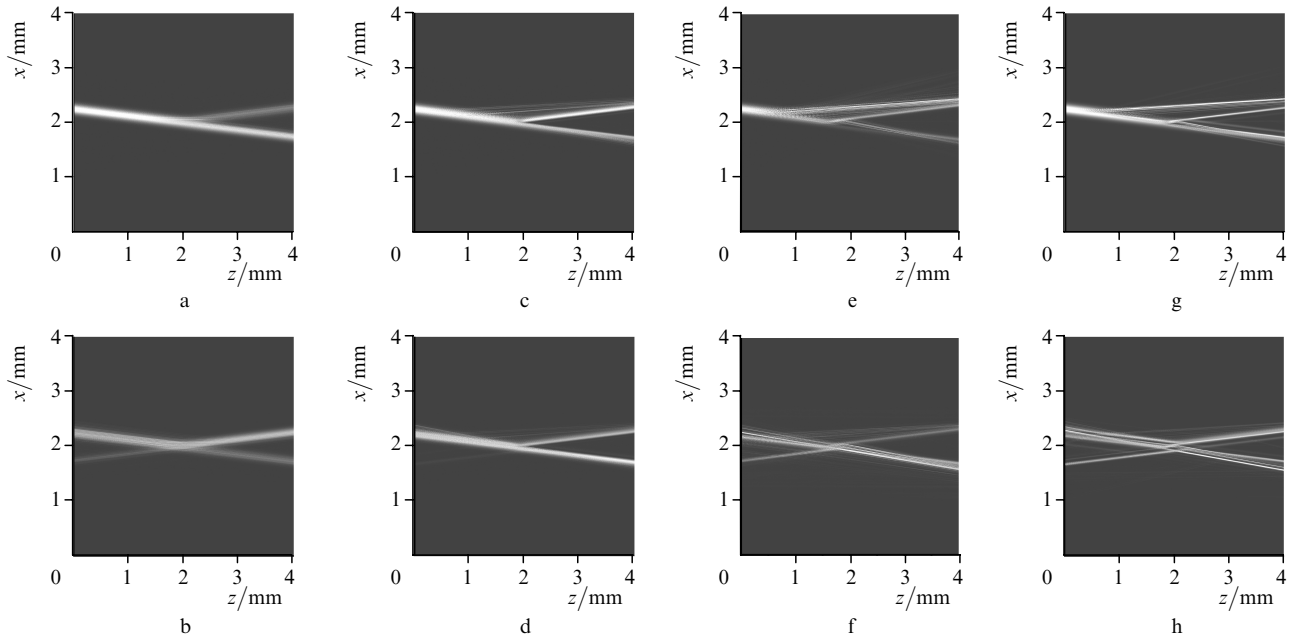

Figure 6. Development of instabilities in the distributions $I_f(x,z)$ (a, c, e, g) and $I_b(x,z)$ (b, d, f, h) at instants $t = 12$ (a, b), 25 (c, d), and 100 s (g, h) for $\alpha = 14^\circ$, $I_{max} = 150$ mW cm^{-2}, $\langle I_n \rangle / I_{max} = 10^{-4}$, and $E_0 = 1$ V cm^{-1}.

which is probably caused by the excess (compared to a single-crystal double PC mirrors) nonlinear phase shifts in the backward wave.

Our calculations confirmed that phase conjugation in self-pumped PC mirrors is also always accompanied by the drastic broadening of the spatial spectrum of the interacting light fields. Taking into account that the energy of the latter is only redistributed among different components of the spatial spectrum, the accuracy of description of high-frequency spatial harmonics proves to be very important. In our case, the required accuracy was realised by using an extremely fine grid steps both along the transverse and longitudinal coordinates (8192 and 512 steps, respectively, for the PRC aperture and length equal to 4 mm). This approach allows us to include the distributed noise into the model and perform similar calculations for other PRC PC mirror schemes.

Our results are in good qualitative agreement with the experimental data. However, we see little reason for attempting to perform any quantitative comparison. The matter is that because all PRCs inevitably contain many defects, the characteristics of crystals even of the same type can differ by more than an order of magnitude. In most experimental papers, all the parameters of PRCs required for simulations were not measured. Therefore, the quantitative interpretation of any real experiment by using our multiparametric microscopic model, whose application, as we have shown, is extremely important for the elucidation of the roles of different characteristics and processes, becomes here a complicated problem.

Acknowledgements. This work was supported by the Program of the President of the Russian Federation on the Support of the Leading Scientific Schools of Russia (Grant No. NSh-1583.2003.2).

References

1. Odulov S.G., Soskin M.S., Khizhnyak A.I. *Lazery na dinamihe-skikh reshetkakh* (Dynamic Grating Lasers) (Moscow: Nauka, 1990).
2. Mailhan C. et al. *Phys. Rev. A*, **67**, 023817 (2003).
3. Feinberg J. *Opt. Lett.*, **7**, 486 (1982).
4. Engin D. et al. *Phys. Rev. Lett.*, **74**, 1743 (1995).
5. Gunter P., Huignard J.-P. (Eds) *Photorefractive Materials and Applications. Topics in Applied Physics.* (Heidelberg: Springer, 1988, Vol. 61; 1989, Vol. 62).
6. Voronov A.V., Shuvalov V.V. *Kvantovaya Elektron.*, **34**, 467 (2004) [*Quantum Electron.*, **34**, 467 (2004)].
7. Kukhtarev N.V. et al. *Ferroelectrics*, **22**, 949 (1979).
8. Duree G. et al. *Opt. Lett.*, **19**, 1195 (1994).
9. Vysloukh V.A., et al. *Zh. Eksp. Teor. Fiz.*, **111**, 705 (1997).
10. Vysloukh V.A., Kuzuzov V., Shuvalov V.V. *Kvantovaya Elektron.*, **23**, 157 (1996) [*Quantum Electron.*, **26**, 153 (1996)].
11. Vysloukh V.A., Kuzuzov V., Shuvalov V.V. *Kvantovaya Elektron.*, **23**, 881 (1996) [*Quantum Electron.*, **26**, 858 (1996)].
12. Zozulya A.A. et al. *Phys. Rev. A*, **52**, 4067 (1995).
13. Xie P. et. al. *Appl. Phys. Lett.*, **69**, 4005 (1996); *Phys. Rev. A*, **56**, 936 (1997).
14. Mullen R.A. et. al. *J. Opt. Soc. Am. B*, **9**, 1726 (1992).